Nanometric-sized Fe/Pt thin films with perpendicular anisotropy developed by layer-by-layer pulsed lased deposition

C. Constantinescu[1], E. Morintale[1,2], N. Scarisoreanu[1],
A. Moldovan[1], M. Dinescu[1]

[1]INFLPR - National Institute for Laser, Plasma and Radiation Physics, PPAM - Lasers

Department, 409 Atomistilor blvd., Magurele, RO-077125, Bucharest, Romania

[2]University of Craiova, Faculty of Physics, 13 A.I. Cuza St., Craiova, RO-200585,

Dolj, Romania

Abstract

Continuous Fe/Pt thin films were fabricated on double-polished silicon and platinum covered silicon plates from elemental Fe and Pt targets at room temperature and in high vacuum (10^{-6}mbar), by using a pulsed Nd:YAG laser working at 266 nm wavelength. The structure and magnetic properties of the films were characterized by atomic force microscopy, X-ray diffractometry and vibrating sample magnetometry. As the film thickness increases, the coercivity increases, while the remanent magnetization and saturation magnetization decrease, showing potential in hard magnetic applications.

Keywords: thin films, Fe/Pt, PLD.

1   Introduction

As magnetic recording density increases to ultra-high density (>1 Tbit/in^2), the grain size of thin-film recording media must be very small. Perpendicular magnetic recording (PMR) including heat assisted magnetic recording has been considered as a promising way to achieve the recording areal density. But the thermal fluctuation may overcome the magnetic anisotropy energy and disarrange the magnetic moments of the recording bits. This phenomenon is known as the superparamagnetic effect. Patterned media have been suggested as a potential solution for this physical limit [1]. Stoichiometric Fe/Pt intermetallic alloy with L1$_0$ ordered structure Figure (1) is considered as one of the leading candidate materials for the next generation of the ultrahigh-density magnetic recording media, because of its large magnetocrystalline anisotropy constant ($\sim 7 \times 106$ J/m^3), small grain size (about 3 nm) permitting thermal stability, high coercivity and excellent corrosion resistance [2]. Fe/Pt alloys have been investigated over the past decades because they have attracted much attention as materials for special permanent magnet application and for ultra-high density magnetic recording [3], [4]. However, Fe/Pt thin films deposited at room temperature adopt a disordered face-centered cubic (fcc) structure with soft magnetic properties. Fe/Pt films presents the shape memory effect [5] and invar effect [6].

The degree of chemical ordering can be enhanced by lowering the deposition rate for the Fe/Pt layers. A slow deposition process also promotes the formation of the (001)
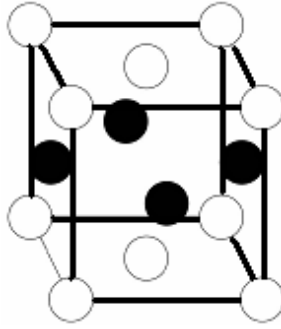
Figure 1: Schematic of the $L1_0$ unit cell: ● represents the A-sublattice and ○ is the B-sublattice [12].

preferred orientation by improving epitaxial growth, because the thickness of the Fe and Pt layers in each revolution become smaller as the deposition rate is reduced. Therefore, the diffusion lengths of Fe and Pt atoms required for migration into the lattice sites become shorter.

There are several new technologies that involve $L1_0$ Fe/Pt of which most important are thin films for improved conventional hard disc drives, or monodisperse Fe/Pt nanoparticles deposited with variety of techniques for patterned data storage media. Despite the substantial development of deposition techniques effective application of the materials still faces a number of problems, one of which is that the monodisperse Fe/Pt particles show no atomic long-range order. Although $L1_0$ ordering occurs on annealing, the treatment causes a parasitic effect of particle sintering and coalescence. Recent results of both experimental studies and computer simulations are consistent about the fact that in the ordered $L1_0$ nano-particles or nano-layers free surface causes a decrease of the superstructure stability. However, there is still an open discussion about the atomistic origin of the observed behaviour.

Recent Monte Carlo simulations suggested the explanation either in terms of substrate-thin film buffer layer, surface Pt precipitation (in large particles and films the thickness of the resulting Pt layer is sufficient to strongly impede oxidation, while in small particles this layer is incomplete and no longer provides protection against oxidation), surface Fe oxidation (metallic nanoparticles containing 3d elements are generally susceptible to oxidation leading to a deterioration of desired properties), or in terms of surface-induced disorder [7] - [14].

2   Experimental

2.1   The PLD technique

The first laser was succesfully run on May 16th in 1960 by *Theodore Maiman* at the Hughes Research Laboratory in California, by shining a high-power flash lamp on a ruby rod with silver-coated surfaces [15]. In 1965, lasers have been used for the first time in thin film deposition experiments when *H.M Smith* şi *A.F Turner* ablated material from a target in a low pressure chamber, by usind a ruby laser, but the thin films were not perfectly uniform in thickness and did not adhere to the substrate [16]. During the next two decades, however, laser ablation was mainly used for the analysis of various materials and further development of PLD was slow. The turning point in PLD applications was
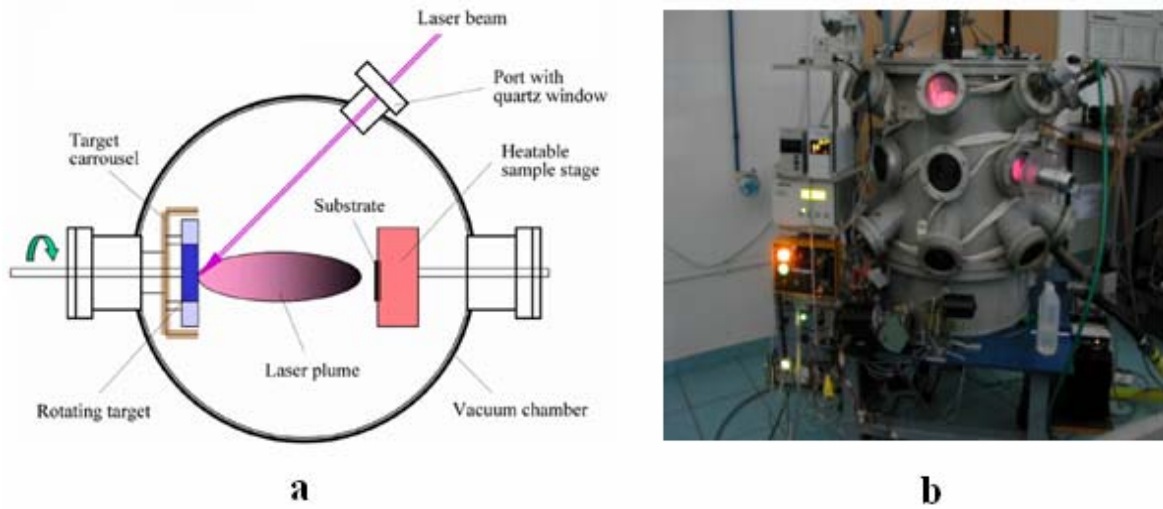
Figure 2: Schematic of the pulsed laser ablation technique (a) and photograph of the experimental setup (b) [22].
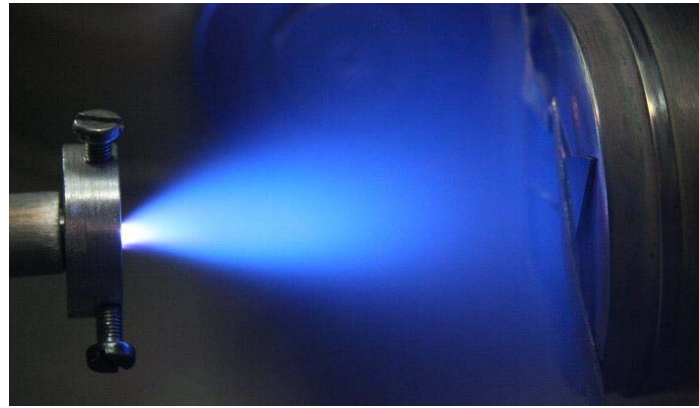

Figure 3: Photograph of a plasma plume during the PLD procedure

the development of YBCO superconductor thin films by *Dijkkamp et al.* in 1987 [17], such that from that point on, and also due to the development of high power, pulsed laser sources that give nano-, pico- and femto-second pulses, the laser ablation technique was improved and other laser-assisted techniques were developed, such that nowadays there is an impressive number of applications that include: mass spectrometry, UV lithography, production of free atoms for laser spectroscopy, and inertial confinement fusion research in the future.

The principle of laser ablation is illustrated in Figure(2 a) while a typical ablation plume is presented in Figure (3). The basic idea of the technique is to exploit high-power laser pulses, e.g., a Nd:YAG (or another similar laser), in order to evaporate a small amount of matter from a solid target [18] - [22].

A laser beam from a "Surelite II" pulsed Nd:YAG laser system (Continuum Company) working at 266 nm wavelength, 10 Hz repetition rate, 7 ns pulse duration and at an incident fluence in the range of 2.5 – 4 J cm^{-2} was used for the experiment.

The substrates, square plates ($\sim$1 cm^2) of double-polished silicon and platinum covered silicon (500 nm Pt thickness with a 20 nm Ti buffer layer, produced by Siegert Consulting

Figure 4: Schematic of the atomic force microscope principle (a) and actual images of the microscope setup (b and c).

e.K.), were placed at a distance of 4 cm from the target; these were firstly cleaned in an ultrasonic bath for 15 minutes, using acetone and isopropanol as cleaning mediums, then dried under pressured nitrogen gas flow. The substrates were held at room temperature during the deposition experiments. In order to have uniform ablation the Fe and Pt targets were rotated and the laser beam scanned the targets surfaces, with 10 laser pulses for each target. Several series of samples were developed in order to test the influence of deposition conditions on the texture, roughness, composition and magnetic properties.

2.2 Thin film characterization techniques

Atomic force microscopy (AFM) is a very high-resolution type of scanning probe microscopy, with demonstrated resolution of fractions of a nanometer, more than 1000 times better than the optical diffraction limit. The AFM consists of a cantilever with a sharp tip (probe) at its end that is used to scan the specimen surface. The cantilever is typically silicon or silicon nitride with a tip radius of curvature on the order of nanometers. When the tip is brought into proximity of a sample surface, forces between the tip and the sample lead to a deflection of the cantilever according to Hooke's law. Depending on the situation, forces that are measured in AFM include mechanical contact force, van der Waals forces, capillary forces, chemical bonding, electrostatic forces, magnetic forces, Casimir forces, solvation forces, etc. As well as force, additional quantities may simultaneously be measured through the use of specialized types of probe. Typically, the deflection is measured using a laser spot reflected from the top surface of the cantilever into an array of photodiodes Figure (4a). Other methods that are used include optical interferometry, capacitive sensing or piezoresistive AFM cantilevers. These cantilevers are fabricated with piezoresistive elements that act as a strain gauge. Using a *Wheatstone bridge*, strain in the AFM cantilever due to deflection can be measured, but this method is not as sensitive as laser deflection or interferometry. Fe/Pt thin films surface aspect and roughness were analysed by AFM using a "Nomad" setup produced by "Quesant Instrument Corporation" Figure (4b) and Figure (4c).

A vibrating sample magnetometer (VSM) is a scientific instrument that measures magnetic properties. A magnetic sample is placed inside a uniform magnetic field to magnetize the sample. The sample is then physically vibrated sinusoidally, typically through the use of a piezoelectric material Figure (5a). Commercial systems use linear
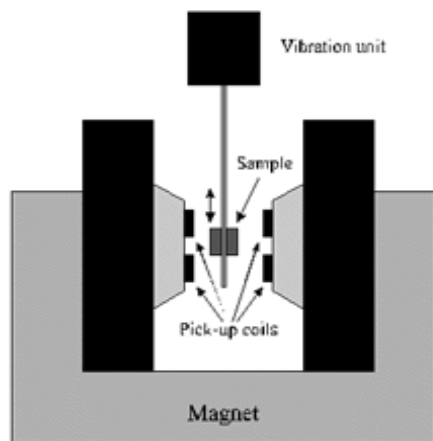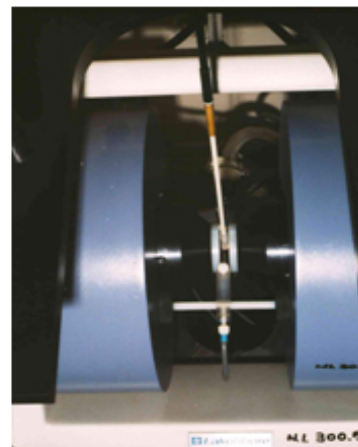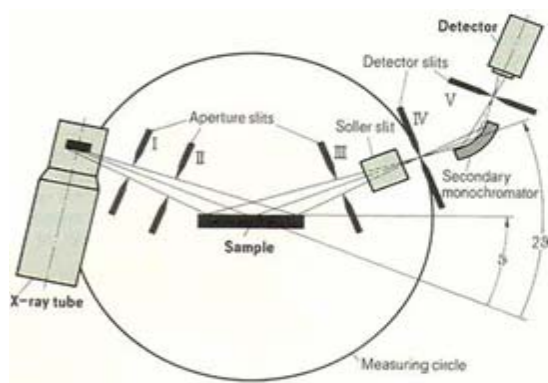
Figure 5: Schematic of the VSM principle (a) and actual image of the LakeShore setup (b).

Figure 6: Schematic of the XRD principle (a) and actual image of the DRON DART UM2 setup (b).

attenutators of some form and historically the development of these systems was done using modified audio speakers, though this approach was dropped due to the interference through the in-phase magnetic noise produced, as the magnetic flux through a nearby pickup coil varies sinusoidally. The induced voltage in the pickup coil is proportional to the sample's magnetic moment, but does not depend on the strength of the applied magnetic field. In a typical setup, the induced voltage is measured through the use of a lock-in amplifier using the piezoelectric signal as its reference signal. By measuring in the field of an external electromagnet, it is possible to obtain the hysteresis curve of a material. Vibrating sample magnetometry was performed for specific magnetic characterization on a LakeShore setup Figure (5b).

X-ray crystallography is an important method of determining the arrangement of atoms within a crystal in which a beam of X-rays strikes a crystal and diffracts into many specific directions. If X-rays of known wavelength strike a crystal whose lattice planes are separated by a distance d, the radiation will be strongly reflected at angles which satisfy Bragg's Law:

$$\lambda = 2d \sin \theta$$

When the values of θ and 2θ are known, the corresponding values of d can be calculated. Using the calculated values of d it is possible to extrapolate a great deal of information about the sample: from the angles and intensities of these diffracted beams, a crystallographer can produce a three-dimensional picture of the density of electrons within the crystal. From this electron density, the mean positions of the atoms in the crystal can be determined, as well as their chemical bonds, their disorder and various other information (qualitative and quantitative mineral content, crystallographic structure determination, identification of unknown substances). Figure (6a) shows a common configuration for an XRD unit. Full featured units are upgradeable with additional hardware to optimize the instrument for single thin film measurements, crystal analysis, high speed diffraction scanning, high resolution diffraction, bath ratio and many other special applications. Bench-top models are available, however, their functionality is severely limited making them extremely inflexible and narrow in their area of application. For this experiment a DRON DART UM2 diffraction setup was used, presented in Figure (6b).

3 Results and discussion

3.1 The AFM technique

The AFM images of the Fe/Pt samples are presented in Figure (7). The surface of the samples appear to be uniformly covered and relatively smooth Figure (7a), with only small droplets present on the surface Figure (7b) and Figure (7c); the root mean square deviation (RMS deviation) is 8.025 nm. As an extrinsic property the coercivity of a thin film strongly depends on the internal and, more impotant, the surface microstructure but this aspect is to be detailed when the magnetic properties of the Fe/Pt samples are discussed.

3.2 The XRD technique

In Figure (8) it is shown the XRD pattern of as-deposited Fe/Pt thin films. The thin films exhibit peaks of disordered face-centered cubic (fcc), but also ordered face-centered tetragonal (fct) planes (001) at about 21^0 and (111) at about 38^0; the dominant phase is the fct Fe/Pt phase. The intensities of the Fe/Pt (001) peak increases as Fe/Pt thickness
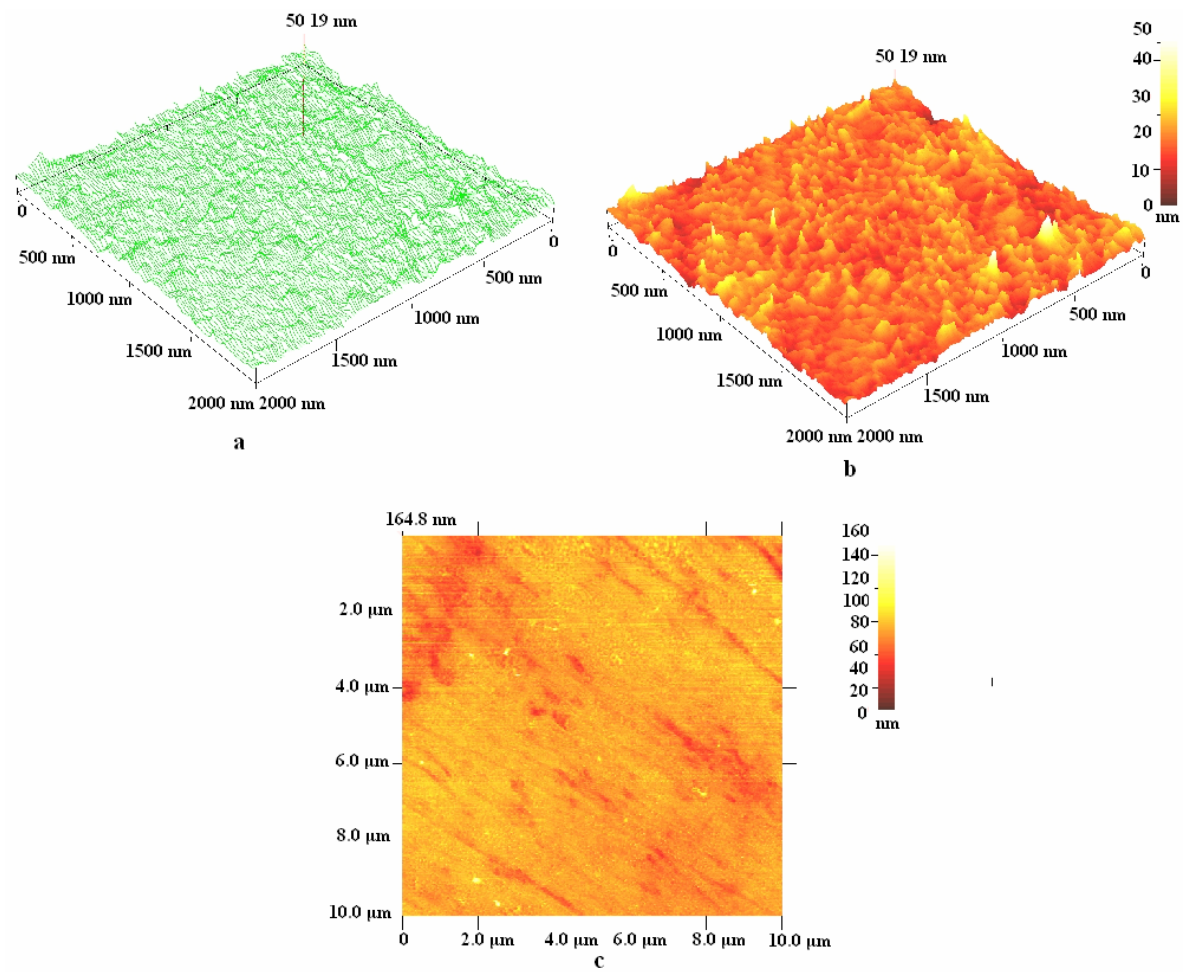
Figure 7: AFM images of the thin film surface (RMS deviation: 8.025 nm): $2\mu m^2$ 3D shape lines (a) and surface characteristics (b); $10\mu m^2$ 2D image of a thin film (c).
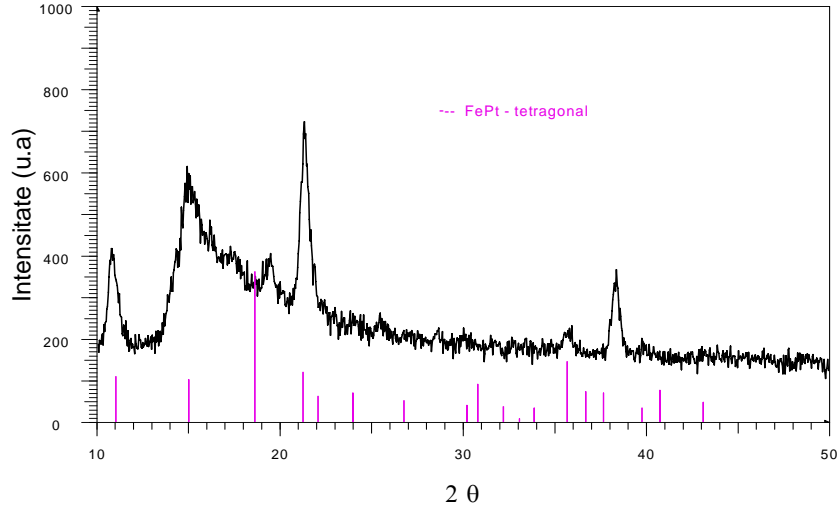
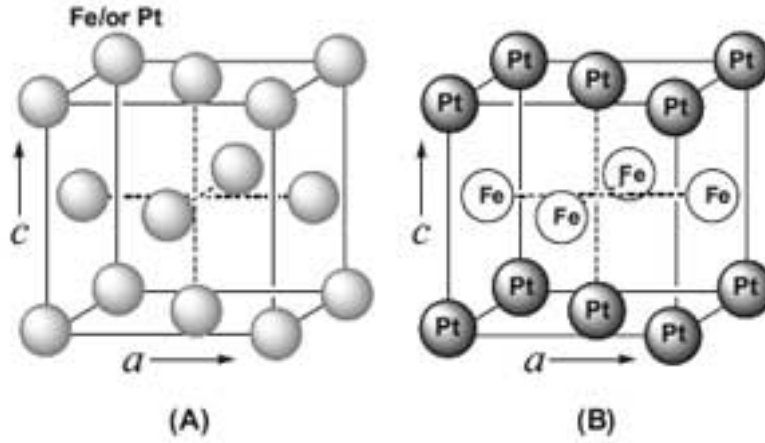Figure 8: XRD spectrum of the Fe/Pt as-deposited thin films.

Figure 9: Schematic illustration of the unit cell of (A) chemically disordered fcc and (B) chemically ordered fct Fe/Pt (b) (source of the images: Brown University).

increased to at least 10 nm. The origin of fct Fe/Pt (001) texture evolution in the films was due to the occurrence of anisotropic strain during ordering transformation [2], [7], [8], [23], [24]; a schematic is presented in Figure (9). Thus, the Fe/Pt (001) texture could be obtained by PLD of atomic-scale layer of Fe and Pt deposition.

3.3   The VSM technique

Perpendicular magnetic anisotropy (PMA) was observed in the films after at least 15 repetitions (N = 15) of Fe/Pt deposition [24] - [27]. A steady increase in the coercive field (H_C) was found with an increase in the number of bilayers from 5 to 16 but then H_C levels off for N > 16. The latter can be attributed to an increase in the number of structural defects with increasing bilayer number affecting the interface quality and thus eventually resulting in an overall reduction of the magnetic anisotropy [25]. The droplets observed by AFM may be a source of magnetic pinning in domain magnetization reversal, which can lead to a (small) increase in thin film coercitivity, but the actual origin of this
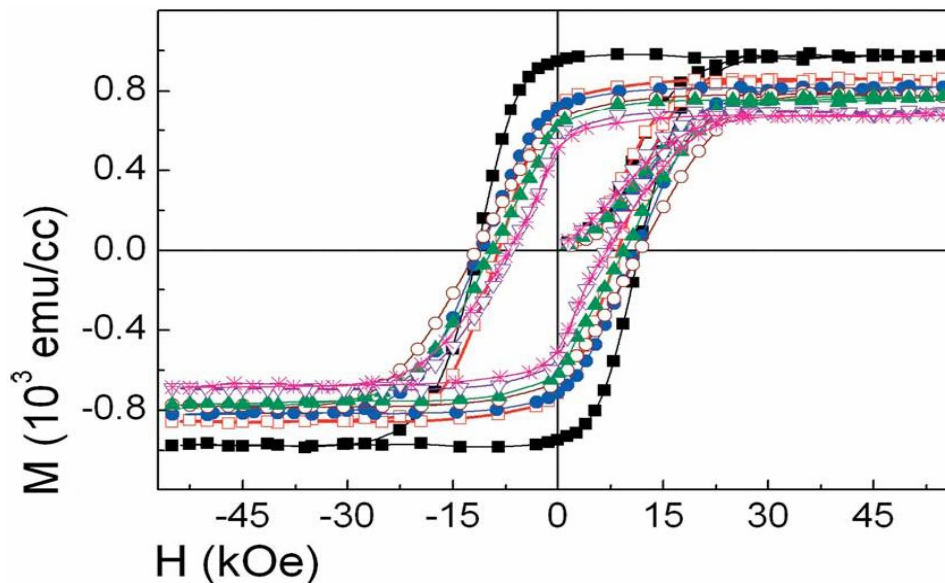
Figure 10: Hysterezis loops measured in the out-of-plane geometry for the FePt thin films deposited at room temperature [10].

enhancement of the coercive field is not yet completly clear.

Several hysterezis loops of the Fe/Pt samples are presented in Figure (10). Such a perpendicular magnetic anisotropy could improve the writability and signal-to-noise ratio in magnetic recording media.

4   Conclusions

Pulsed laser-assisted deposition techniques are clean, simple yet versatile methods that allow good control in thin films and/or multilayer-structured samples. We have prepared and investigated the magnetic properties and microstructures of nanometer-size Fe/Pt films on silicon and platinum covered silicon substrates, at room temperature. The surface morphology of the films reveal a relatively smooth surface with only few small (under 50 nm) droplets. The XRD patterns reveal the crystalline structure of the films, while the VSM measurements show that perpendicular anysotropy is present.

References

[1] N. Honda, S. Takahashi, K. Ouchi, J. Magn. Magn. Mater. 320 (2008) 2195.

[2] Y.S. Yu, Hai-Bo Li, W.L. Li, Mei Liu, Yu-Mei Zhang, W.D. Fei, D.J. Sellmyer, Thin Solid Films 518 (2010) 2171.

[3] S. Sun, C.B. Murray, D.Weller, I. Folks, A. Moser, Science 287 (2000) 1989.

[4] L.C. Varanda, M. Jafelicci Jr., M. Imaizum, J. Appl. Phys. 101 (2007) 123918.

[5] S. Fujji, S. Ishida, S. Asano, J. Phys. Soc. Jpn. 59 (1989) 3657.

[6] M. Imaizumi, C.A. Soufen, C.A.F. Pintão, L.C. Varanda, M. Jafelicci Jr., Mat. Sci. Eng. A 521–522 (2009) 167.

[7] G.P. Lin, P.C. Kuo, K.T. Huang, C.L. Shen, T.L. Tsai, Y.H. Lin, M.S. Wu, Thin Solid Films 518 (2010) 2167.

[8] P. Schaaf , K. Zhang, C. Lange, A. Holz, M. Weisheit, S. Fahler, Appl. Surf. Sci. 253 (2007) 8107.

[9] L.J. Qiu, J. Ding,A.O. Adeyeye, J.H. Yin, J.S. Chen, S. Goolaup, N. Singh, IEEE Trans. Magn. 43 (2007) 2157.

[10] A. Perumal, Y. K. Takahashi, K. Hono, J. Appl. Phys. 105 (2009) 07B732.

[11] Z.H. Lu, M.J. Walock, P. LeClair, W.H. Butler, G.J. Mankey, J. Vacuum Sci. Tech. A 27 (2009) 1067.

[12] L.Y. Han, U. Wiedwald, B. Kuerbanjiang, P. Ziemann, Nanotechnology 20 (2009) 285706.

[13] S.W. Wang, A.C. Sun, F.T. Yuan, J.H. Hsu, P.C. Kuo, IEEE Trans. Magn. 45 (2009) 3580.

[14] M. Koz1owski, R. Kozubski, Ch. Goyhenex, V. Pierron-Bohnes, M. Rennhofer, S. Malinov, Intermetallics 17 (2009) 907.

[15] T. H. Maiman, Phys. Rev. Lett. 4 (1960) 564.

[16] H. M. Smith, A. F. Turner, Appl. Opt. 4 (1965) 147.

[17] D. Dijkkamp, T. Venkatesan, X. D. Wu, S. A. Shaheen, N. Jisrawi, Y. H. Min-Lee, W. L. McLean, M. Croft, Appl. Phys. Lett. 51 (1987) 619.

[18] J. C. Miller (editor), "Laser Ablation - Principles and Applications", Springer-Verlag, Berlin, 1994.

[19] D. B. Chrisey, G. K. Hubler (editors), "Pulsed Laser Deposition of Thin Films", John Wiley & Sons Inc., New York, 1994.

[20] D. B. Chrisey, R.W. Eason (editors), "Pulsed Laser Deposition of Thin Films: Applications in Electronics, Sensors, and Biomaterials", John Wiley & Sons Inc., New York, 2007.

[21] M. von Allmen, A. Blatter (editors), Laser-Beam Interactions with Materials, Springer-Verlag, Berlin, 1995.

[22] www.physandtech.net

[23] Z.Y. Pan, R.S. Rawat, J.J. Lin, T. Zhang, P. Lee, T.L. Tan, S.V. Springham, Appl. Phys. A 96 (2009) 1027.

[24] S. Sun, Advanced Materials 18 (2006) 393.

[25] D. Makarov, J. Lee, C. Brombacher, C. Schubert, M. Fuger, D. Suess, J. Fidler, M. Albrecht, Appl. Phys. Lett. 96 (2010) 062501

[26] J.Y. Ahn, N.J. Lee, T.H. Kim, J. Magn 14 (2009) 144.

[27] J.L. Tsai, H.T. Tzeng, G.B. Lin, Appl. Phys. Lett. 96 (2010) 032505.